Water Exchange around Li^+ and Na^+ in LiCl(aq) and NaCl(aq) from MD Simulations

Kersti Hermansson* and Mark Wojcik

Inorganic Chemistry, The Ångström Laboratory, Uppsala University, Box 538, S-751 21 Uppsala, Sweden

Received: October 24, 1997

The solvent exchange mechanisms around alkali cations in dilute aqueous solution have been investigated from cation−oxygen distance vs time curves, molecular animations, activation volumes, and lifetime statistics. Constant pressure (0 atm)−constant temperature (300 K) MD simulations were performed for two LiCl(aq) solutions and one NaCl(aq) solution. The two LiCl(aq) solutions had different ionic charges, ±1.0 and ±0.8. The TIP4P water−water potential combined with Bounds's ion−water potentials were used. Most of the exchange processes can be classified in terms of dissociative (D), associative (A) or interchange type mechanisms: I_D, I, or I_A. Many exceptions are found in the NaCl(aq) solution, where ∼10% of the exchanges are of a more elaborate nature, although the majority are associative. Around the lithium ion, the exchanges are dissociative (D and I_D). The exchange rate in NaCl(aq) is much higher than in LiCl(aq). The activation volumes for the 6-5-6 [LiCl(aq)] and 6-7-6 [NaCl(aq)] exchange processes were calculated by two methods: from cation-H radial density distribution curves for the 5-, 6-, and 7-complexes, and from the volumes of Voronoi polyhedra. Both methods give a negative $\Delta V^{\ddagger}$ for the associative process and a positive $\Delta V^{\ddagger}$ for the dissociative process, supporting a mechanistic interpretation of the sign of $\Delta V^{\ddagger}$.

1. Introduction

Because the vast majority of chemical and biological processes take place in aqueous media, such ionic solutions have always attracted great scientific interest. In solution, solvent and ligand exchange behavior is important for most chemical processes. The pure solvent exchange reaction for a hexahydrated metal ion in water can be formulated as

$$M^{n+}(H_2O)_6 + H_2O^* \rightarrow M^{n+}(H_2O)_5H_2O^* + H_2O \quad (1)$$

Much is already known about the hydration structure around metal ions in solution from diffraction experiments, NMR and infrared spectroscopy techniques.[1] Much less detailed information exists concerning the *dynamics* of solvated ions in solution. Ion diffusion has been measured by various experimental methods such as electrochemical measurements, NMR, and QENS (quasi-elastic neutron scattering). Even less is known about the detailed microscopic dynamics of the solvent molecules around the ions. Rate constants for water exchange around metal cations have been measured using NMR and are found to span an enormous range: residence times of the order of picoseconds for the alkali ions up to several days for Rh^{3+}.[2,3] For the very fast exchange processes around alkali cations, experimental data is not very precise.

Some quantum-mechanical ab initio studies of exchange mechanism have appeared. Veillard[4] calculated the hydration number and hydration energy of Al^{3+}(aq) and Cu^{2+}(aq) and proposed the S_N1 mechanism for the exchange of water molecules between the first and second hydration spheres around Al^{3+}. Probst and Hermansson[5] computed binding energies for energy-minimized $M^{n+}(H_2O)_m$ ($M^{n+} = Li^+$, Na^+, Mg^{2+}, and Al^{3+}; $m = 5, 6, 7$) and found that, for the latter three ions, the formation of the 5-complex was energetically more favourable than the formation of the 7-complex. Åkesson et al. computed binding energies of the sixth ligand[6] and of an added seventh ligand[7] for hexahydrated divalent first-row transition metal ions from Ca^{2+} to Zn^{2+}. More recently, Rotzinger[8] computed the structures of the transition states and of intermediates for water exchange around Ti^{3+}, V^{2+}, and Ni^{2+}; here it was not possible to distinguish energywise between the D and I_A mechanisms (see below). All these studies indicate that it is not an easy task to determine the exchange mechanism from isolated-cluster ab initio calculations.

In the present work we make an attempt to analyze, classify, and compare the mechanisms for water exchange around a Li^+ ion and a Na^+ ion in dilute aqueous solutions by means of constant pressure−constant temperature MD simulations. Earlier, MD studies of residence times and exchanges of water molecules in the first hydration shell of alkali cations have been reported in the literature (see, for example, refs 9−13). We know of only a small number of previous MD studies where exchange *mechanisms* around metal ions in water are discussed. Kowall et al.[14,15] have made detailed mechanistic studies of hydrated Ln^{3+} ions using MD simulations. The exchange rate of water molecules around Na^+(aq) was studied in MD simulations by Rey and Hynes,[16,17] who observed both S_N1 (unimolecular, dissciative) and S_N2 (bimolecular, associative) type exchanges as well as concerted processes. Our own group recently investigated the effect of pressure on the exchange mechanisms for Na^+(aq).[18]

We have also studied the so-called activation volume, which experimentally is defined from the pressure dependence of the rate constant, k_{expt}: $(\partial \ln k_{expt})/\partial P|_T = -\Delta V^{\ddagger}_{expt}/RT$.[19,20] A negative $\Delta V^{\ddagger}_{expt}$ thus corresponds to a rate increase with increasing pressure, and a positive sign indicates a rate decrease. In the literature, relying on concepts from transition-state theory, the activation volume has been interpreted at the molecular, mechanistic level as the difference between the volume of the transition state and the volume of the complex in its initial state.

* Corresponding author. E-mail: kersti@kemi.uu.se.

S1089-5647(97)03465-2 CCC: $15.00
Published on Web 07/11/1998

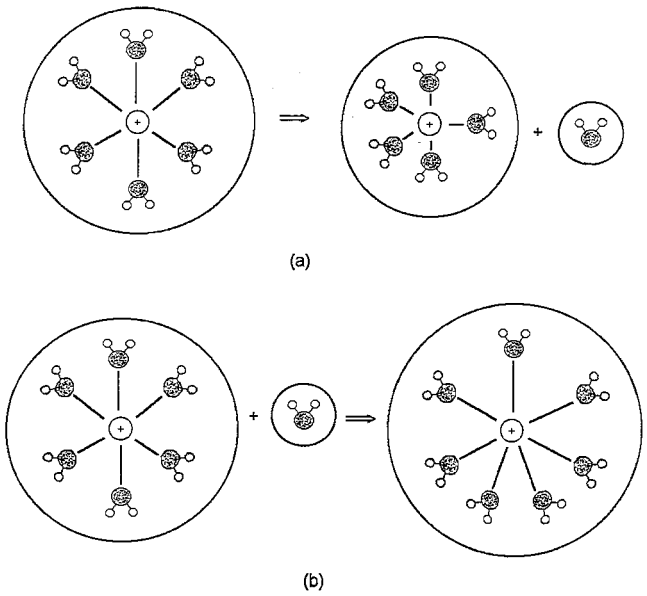

Figure 1. Schematic view of activation volume changes. (a) The change going from the 6-coordinated complex to the 5-coordinated intermediate, i.e., the dissociative mechanism. (b) The change from a 6-coordinated to a 7-coordinated complex, i.e., the associative mechanism.

A negative $\Delta V^{\ddagger}_{expt}$ has been interpreted as evidence of an associative mechanism, and a positive volume as evidence of a dissociative mechanism. In the present paper, we have computed molecular-level activation volumes to try to verify whether such a mechanistic interpretation of $\Delta V^{\ddagger}$ is reasonable. We do not know the exact transition states in the different exchange situations that arise in our aqueous solutions, and instead we use the intermediate 5- and 7-complexes to estimate $\Delta V^{\ddagger}$. This is depicted schematically in Figure 1. The activation volume is actually defined in terms of differences between partial molar volumes. However, following Burgess,[19] we will make the tacit assumption that the electrorestriction effect is similar for the hexacoordinated complex and the activated complex, allowing us to discuss volumes instead.

Morita et al.[21] computed the molecular activation volume for model ionic reactions $A^+ + B^- \Rightarrow$ products in water via the "reference linearized hypernetted chain theory" of fluid structure, from calculations at several pressures. Here we have calculated the activation volume without changing the pressure, that is to say, just from the geometries of the activated complexes and their surroundings in the zero-pressure solution. Kowall et al.[15] have calculated activation volumes for water exchanges around Ln^{3+}, using a different space-partitioning scheme than ours. They also estimated the activation volume from the pressure dependence of the equilibrium constant between the different hydration complexes.

The outline of the paper is as follows. After the methods section, the thermodynamical and structural results will be given in the first two parts of the results section. The last three parts deal with the exchange mechanisms, the intermediate complexes, and calculation of the activation volume.

2. Computational Details

The MD Simulations. MD simulations at constant temperature (300 K) and constant pressure (0 atm) were performed for three systems: two LiCl(aq) solutions with different ionic charges and one NaCl(aq) solution. The equations of motion for the box were treated by Anderson's "pulsating box" method.[22] The Nosé−Hoover formalism[23] was used for the constant temperature control. Electrostatic interactions in the system were treated by the Ewald method, as adapted to rigid molecules in a pulsating box by Nosé and Klein.[24] In all cases, the MD box consisted of 123 rigid water molecules and one ion pair, giving solution concentrations of 0.443 mol/kg for the two LiCl(aq) solutions and 0.440 mol/kg for NaCl(aq). Using the average box volumes given in Table 1, the molar concentrations come out to 0.463, 0.460 and 0.460 mol/L, respectively. Each simulation was equilibrated for about 7.5 ps and then run for about 2.5 ps before data collection was started. The data collection was in all cases ∼300 ps. The time step used was 0.75 fs. The configurations (molecular coordinates, velocities, and accelerations) were dumped to disk every 10th time step.

The Interatomic Potentials. The simulations performed here used Jorgensen's potential for pure bulk water, TIP4P.[25] TIP4P places a charge of $+0.52e$ on each hydrogen atom, a charge of $-1.04e$ 0.15 Å away from the oxygen toward the hydrogens, and a non-Coulombic site on the oxygen of type $a/r^{12} - b/r^6$, where r is the distance between the oxygen atoms on two water molecules. The O−H distance is 0.9572 Å and the H−O−H angle is 104.52°. The Li^+-H_2O, Na^+-H_2O, and Cl^--H_2O potentials were taken from Bounds.[26] The Li^+-Li^+, Li^+-Cl^-, Cl^--Cl^-, Na^+-Na^+, and Na^+-Cl^- were taken from ref 27.

In spite of the fact that the exchange rates of water molecules around the alkali ions are very fast ($t_{1/2} = \sim 1$ ns), compared to many other ions ($t_{1/2}(Al^{3+}) = \sim 1$ s, $t_{1/2}(Cr^{3+}) = \sim 1$ week),[2] it was earlier found in simulations on LiHCOO(aq)[28] that very long simulations must be performed to obtain high statistical precision. Also in the present MD simulations we find only one water exchange around the Li^+ ion in 300 ps. A method to increase the exchange rate around Li^+ was therefore attempted here, namely, to decrease the charge of the ion, so that it cannot hold the water molecules as strongly. In addition to a normal $Li^{+1.0}Cl^{-1.0}$(aq) simulation, a simulation with charges $+0.8e$ for lithium and $-0.8e$ for chlorine was therefore performed. All other potential parameters were left unchanged. We do not claim that this modified lithium−water potential has a sound theoretical basis; it was merely constructed to represent a potential akin to the original potential, but with an enhanced exchange rate. As we will see, both the $Li^{+1.0}$ and the $Li^{+0.8}$ simulations give rise to dissociative exchange processes, and, since the statistics for the latter solution is slightly improved, we use the $Li^{+0.8}$ simulations to study possible mechanistic features of D and I_D type exchanges, and we compute the corresponding activation volume.

For NaCl(aq), both experiment[2] and our current simulations show that the exchange rate of water molecules around Na^+ is much higher than around Li^+, so here the original potential functions were used without modification.

3. Results and Discussion

3.1. Thermodynamic Data. The thermodynamical data from the simulations are collected in Table 1. The density for pure TIP4P-water is 0.999 g/cm^3, and the experimental density is 0.997 g/cm^3, i.e., a difference of ∼0.2%. The TIP4P potential parameters were originally fitted to match the experimental density for pure water.[25] Therefore, it is not surprising that the addition of ions to water increases the discrepancy between the simulated and experimental densities. Here, the differences between the simulated and the experimental densities in the ionic solutions are <∼3%.

3.2. Average Water Coordination around the Cations. Radial distribution functions, $g(r)$, and running integration

TABLE 1: Physical and Thermodymanic Data from the Simulations, Calculated as Averages over the Whole Production Runs

simulation	*P* (MPa)	*T* (K)	pot. *E* (kJ/mol)	total *E* (kJ/mol)	box vol. (Å^3)	density (g/cm^3)	exptl density[30]
LiCl(aq)	0.5(1270)	300.0(16)	−51.1(6)	−43.7(7)	3586(76)	1.05(2)	1.009
$Li^{+0.8}Cl^{-0.8}$(aq)	0.2(1240)	300.0(16)	−48.4(6)	−41.0(7)	3613(79)	1.04(2)	
NaCl(aq)	0.2(1230)	300.0(16)	−49.7(6)	−42.2(7)	3610(80)	1.04(2)	1.017

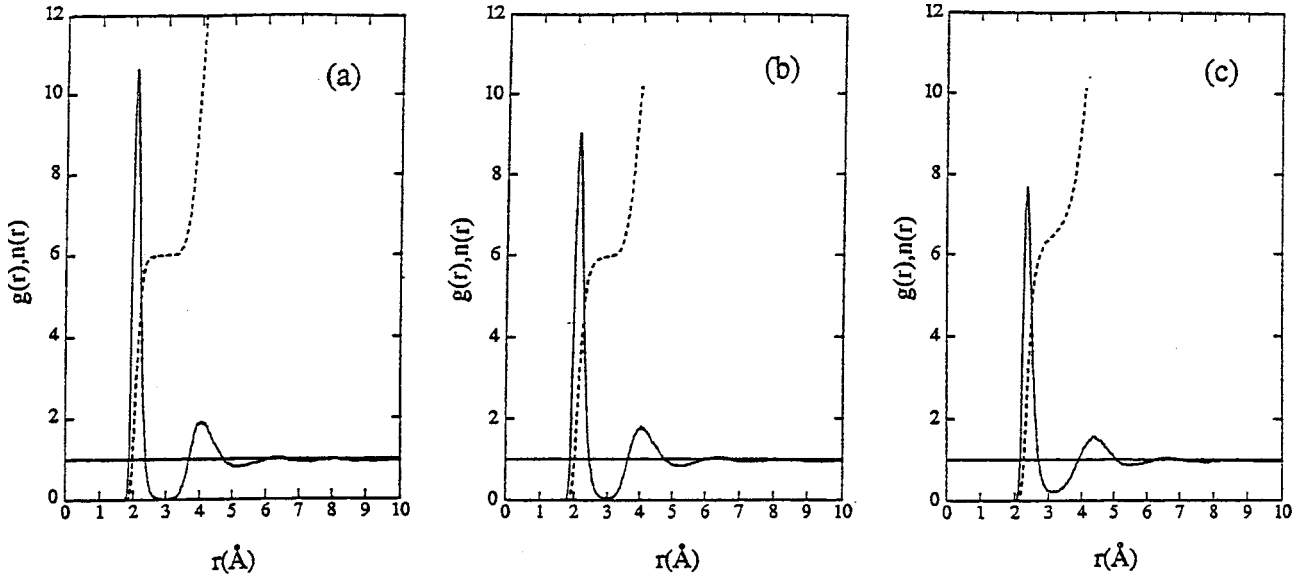

Figure 2. Cation−oxygen radial distribution functions, $g(r)$, and running coordination numbers. The shaded areas are discussed in section 3.3. (a) LiCl(aq). (b) $Li^{+0.8}Cl^{-0.8}$(aq). (c) NaCl(aq).

numbers, $n(r)$, for each simulation were calculated (Figure 2). The $Li^{+1.0}$−O $g(r)$ curve shows a pronounced first hydration shell centered around 2.07 Å. These values are in good agreement with those from (N, V, E) simulations by Bounds[26] using the same potentials. The $n(r)$ value at the plateau between the first and second hydration shells is 6.00. The 2nd shell is centered around 4.06 Å and contains 16.2 water molecules. There is also a weak indication of a third hydration shell.

The $Li^{+0.8}$−O $g(r)$ curve has a first-shell peak maximum at 2.11 Å and the second shell centered around 4.04 Å. The first hydration shell contains 5.97 water molecules, calculated from the $n(r)$ value at the mimimum between the first- and second-shell peaks. The second shell contains 18.6 water molecules. There is also a weak indication of a third hydration shell.

The first hydration shell for Na^+ is centered at 2.36 Å from the sodium ion and the second hydration shell at 4.39 Å. These values are also in good agreement with those from the (N, V, E) simulations by Bounds[24] using the same potentials. The $n(r)$ function does not show the same pronounced plateau-like behavior as for lithium−oxygen. The region between the first and second hydration shells in the cation−oxygen $g(r)$ curves is very close to zero for $Li^{+1.0}$ and $Li^{+0.8}$, but for Na^+ it is clearly above zero. This suggests that there are more exchanges occurring around the sodium ion than around lithium. The $n(r)$ value at the Na^+−O $g(r)$ minimum between the first and second hydration shells is 6.53. The second hydration shell contains ∼20.2 water molecules.

The anion and the cation are generally far apart, as can be seen from their $g(r)$ functions (not shown here). In our simulations, the Cl^- ion resides in the second hydration shells of the cations approximately 2−4% of the total simulation time; otherwise the ions are even further apart. We would have to perform comparative simulations with a much bigger box to be able to discuss with any certitude whether or not the Cl^- ion affects the exchange process around the cations at our current concentration.

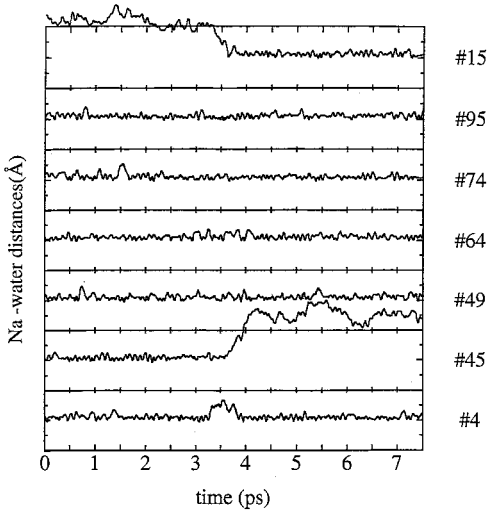

Figure 3. An associative exchange process around the Na^+ ion in the NaCl(aq) solution. The figure shows all seven water molecules that are ever closer than 3 Å to the Na^+ ion within the 7.5 ps long time interval. Water molecule no. 15 enters the first hydration shell; no. 45 leaves. Water no. 4 makes a small excursion into the intershell region, but returns. Such an excursion of a third water molecule is not the rule among the 121 exchange processes observed during this simulation.

3.3. Solvent Exchange Statistics. We have studied the exchange of water molecules around the cation by means of "solvent exchange curves", showing the distances of specific water molecules to the cation as a function of time. Such solvent exchange curves were used to locate all exchanges that take place and to identify which water molecules are involved. Any water molecule that came closer to the cation than 3.0 Å was recorded, and its distance to the cation as a function of time was plotted. This search was repeated throughout the simulations. All exchanges could be pinpointed by this method, and each exchange could be studied closely. One example is shown in Figure 3, where two water molecules change places

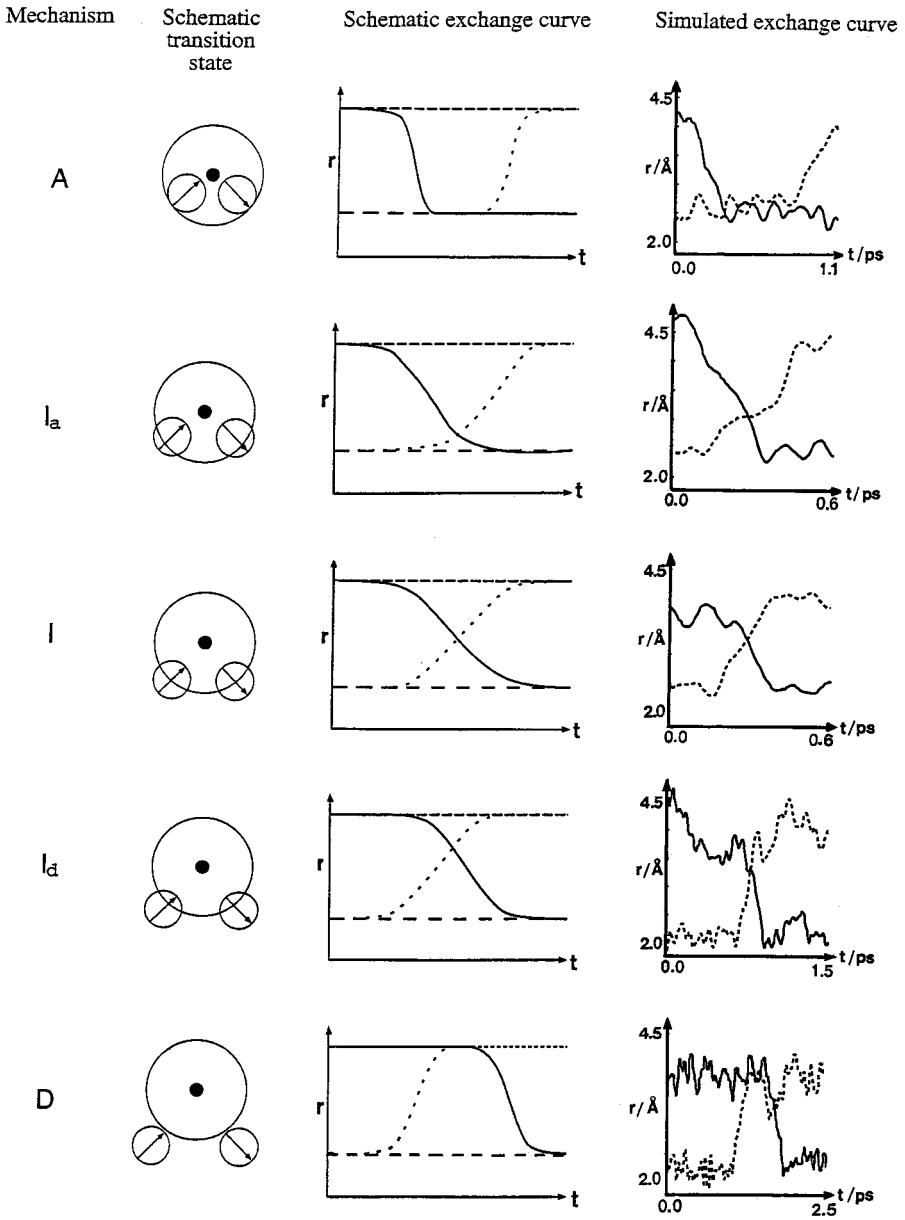

Figure 4. Five exchange processes. First column: classification of prototype exchange mechanism. Second column: Schematic illustration of the exchanges. Third column: cation−oxygen distance exchange curves for the ideal prototype exchanges. Fourth column: Examples of cation−oxygen distance exchange curves from the simulated solutions.

at ∼3.5 ps. The time 0.0 ps is an arbitrarily chosen point in time just before an exchange event.

The water molecules can exchange in a number of ways. In an *associative exchange* (A), an external water molecule first joins the complex, so that the cation becomes coordinated by an additional molecule, before the departing water leaves the complex. In a *dissociative exchange* (D), one water molecule first leaves the complex, before an external water enters. There are also intermediate types of exchange. Both the incoming and the outgoing molecules can exchange at the same time, *interchange* (I), or they can exchange at almost the same time, *associative interchange* (I_A) and *dissociative interchange* (I_D) (see ref 19 and references therein). The third column in Figure 4 shows the solvent exchange curves for these five prototype mechanisms.

Most exchange events found in our simulations could be classified unambiguously as belonging to one of these five mechanisms from the cation−water distance at the crossing point, where the two exchanging water molecules have the same distance to the cation. The last column in Figure 4 shows solvent exchange curves for five "real" examples taken from our MD simulations. For an associative exchange, the crossing point should be close to the typical cation−water distance for water molecules in the first hydration shell. For a dissociative exchange, it should be close to the distance for water molecules in the second hydration shell. We therefore divided the region between the first and second hydration shell $g(r)$ peaks into five equal parts (Figure 5), i.e., between 2.1 and 4.0 Å for the two LiCl(aq) solutions and between 2.3 and 4.35 Å for NaCl(aq). If an exchange happens to occur with a crossing point closer to the cation than the first-shell peak, this is of course also counted as an associative exchange. Likewise, if an exchange has its crossing point further away from the cation than the second-shell peak, it is counted as a dissociative exchange.

An A and an I_D exchange are shown as "animations" in Figure 6. In the associative exchange, the 6-complex starts out as a slightly distorted octahedron, a new water molecule enters, and a pentagonal bipyramid is formed and lives for approximately

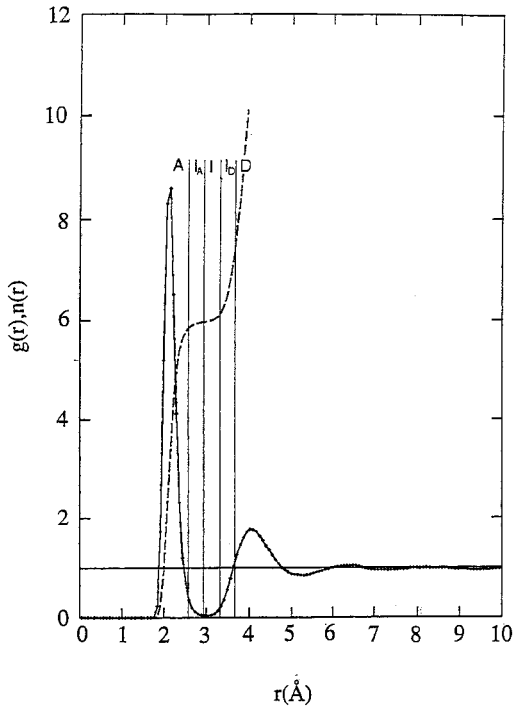

Figure 5. Cation−oxygen distance at the crossing point in the solvent exchange curve (cf. Figure 4), which determined the classification of anexchange as D, I_D, I, I_A or A. The distance range for each of these groups was determined as indicated in the present figure; i.e., the region between the first and second hydration-shell peaks was divided into five parts.

2.5 ps, before "an old" water molecule leaves the complex. In the dissociative interchange exchange, one water molecule leaves the octahedron, and a trigonal bipyramidal intermediate is formed, which goes back to being an octahedral 6-complex after some 0.3 ps.

The solvent exchange curves reveal different mechanisms for the different solutions (Table 2). For LiCl(aq) there are more exchanges of the dissociative type (D and I_D), and for sodium there are more associative exchanges (A and I_A). As far as the exchange rates are concerned, they are seen to differ considerably for LiCl(aq) and NaCl(aq). For the $Li^{+1.0}Cl^{-1.0}$(aq) solution only one single exchange was found during the 300 ps, while for $Li^{+0.8}Cl^{-0.8}$(aq) we found nine events. For Na^+ we found as many as 121 exchange events. This indicates that the Na^+ complex is much more labile than the Li+ complex.

There is a greater variety of exchange mechanisms occurring around the sodium ion. Here it is not sufficient to use the classical five exchange categories. A rather common exchange mechanism in the NaCl(aq) simulations is the associative exchange from a 7- to an 8-coordinated complex and back to a 7-coordinated complex (here called A_{7-8-7}). This mechanism consititutes 5% of the exchange events recorded. Another 13% belong to a manifold of other exchange processes, where often four molecules are involved, exchanging simultaneously or almost simultaneously. These are listed as "others" in Table 2.

The lifetimes of the intermediate complexes were measured from the time when the intermediate complex is fully formed to when it starts to fall apart (Figure 4). The average lifetimes are given in Table 2. Note that we prefer to use the term "intermediate complex" rather than "activated complex" since, at least for the A and D intermediates, the lifetimes are long enough to lead us to assume that these complexes do not represent the highest energy point along the reaction coordinate.

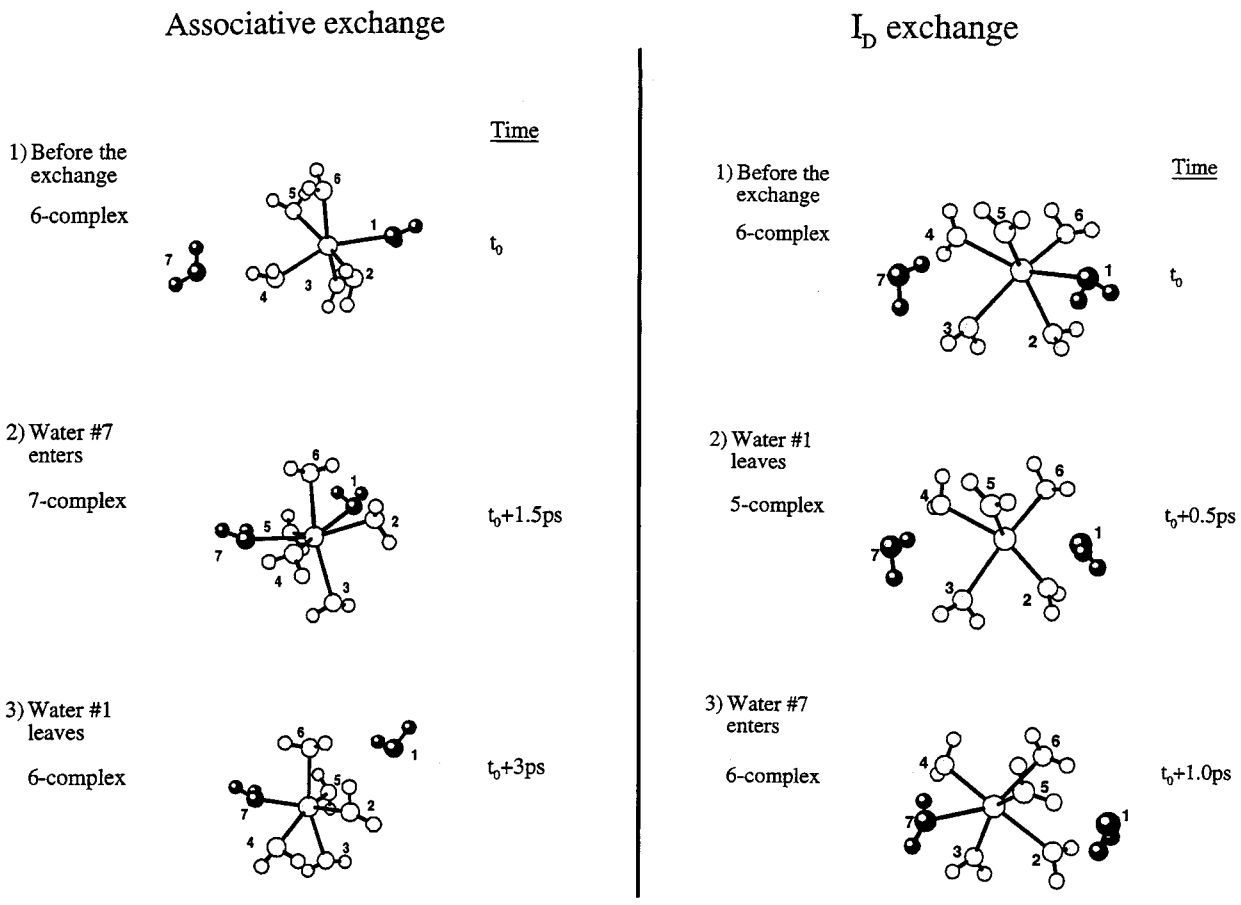

Figure 6. "Animations" of two exchange processes from our simulations.

TABLE 2: Statistical Data on Exchanges and Average Lifetimes of Intermediate Complexes (cf. Section 3.3)[a]

	$Li^{+1.0}$			$Li^{+0.8}$			$Na^{+1.0}$		
exchange type	no. of events	%	average lifetime (ps)	no. of events	%	average lifetime (ps)	no. of events	%	average lifetime (ps)
D	0	0		3	33	0.6(0.3)	0	0	
I_D	1	100	0.03	4	44	0.3(0.3)	0	0	
I	0	0		1	11	0.0	5	4	0.0(0.0)
I_A	0	0		1	11	0.0	9	7	0.0(0.0)
A	0	0		0	0		89	74	0.7(1.0)
A_{7-8-7}	0	0		0	0		5	4	0.2(0.1)
others	0	0		0	0		13	11	0.2(0.1)
total	1	100	0.03	9	100		121	100	0.2(0.1)

[a] The exchange types denoted "others" are exchanges where the crossing-point definition could not be used, i.e., where more than two water molecules change places at the same time.

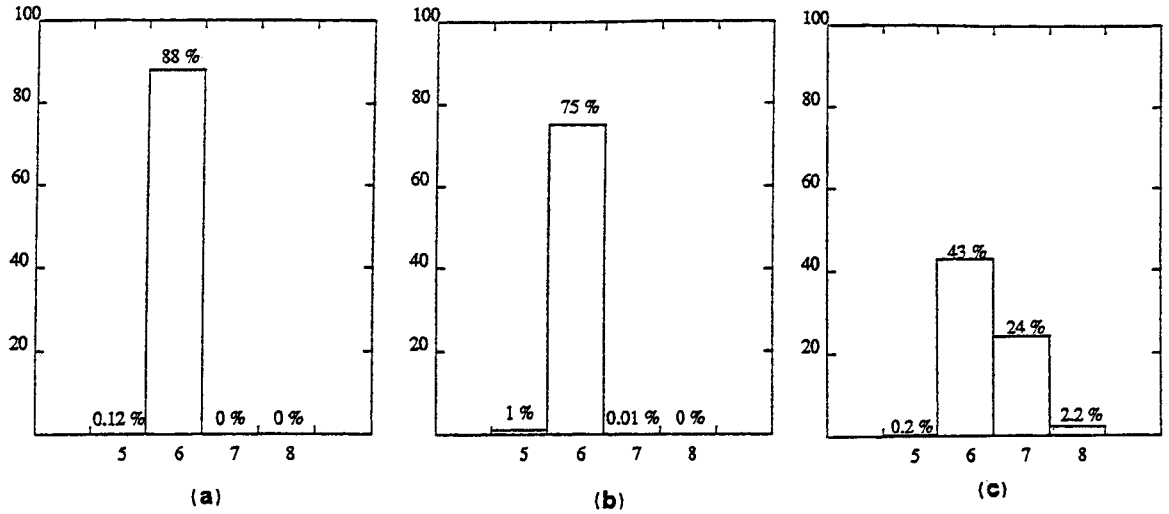

Figure 7. Occurrence of complexes with different coordination numbers in the solutions. The histograms show the probability of finding an *n*-coordinated complex. In all three solutions, the sum of the probabilities for the 5-, 6-, 7-, and 8-complexes amount to less than 100% of all the cation−water configurations analyzed. This is because the remaining complexes have at least one water molecule in the intershell region and were given zero weight in the analysis, as described in the text. (a) LiCl(aq). (b) $Li^{+0.8}Cl^{-0.8}$(aq). (c) NaCl(aq).

The average lifetime of the intermediate 5-complex in the dissociative Li^+ exchange is 0.6 ps. The average lifetime of the intermediate 7-complex in the 6-7-6 exchange around Na^+ is 0.7 ps, and of the intermediate 8-complex in the 7-8-7 exchange 0.2 ps. The range of lifetimes found for a particular mechanism is very large in all three solutions, typically in the range from 0 to 2 ps, with occasional lifetimes as long as 5 ps. The spread in lifetimes is not normally distributed. Moreover, it typically takes ∼0.2−0.5 ps for the intermediate complex to form, i.e., for a a water molecule to leave the first shell and join the second shell or vice versa.

3.4. Coordination Number Statistics. In the analysis of the exchange statistics mentioned above, the occurrences of the 5-, 7-, and 8-intermediates and their lifetimes were recorded. Such complexes can also arise when a water molecule makes *temporary* excursions into or out of the first hydration shell and later returns to its original shell. In this section we present a more complete analysis of the relative occurrences of all intermediate coordination numbers as well as of the 6-complex, taking both exchanges and excursions into account. The probability $P(n)$ of finding an *n*-coordinated cation was thus calculated as

$P(n)$ = (no. of configurations where the cation has a "clean" *n*-coordination)/(total no. of configurations)

Here we wanted to consider only "pure", "integer-coordinated" complexes; therefore, all MD dumps with water molecules residing in the region between the two hydration shells were given a weight of zero in computing $P(n)$. This intershell region was defined to be where the cation−oxygen $g(r)$ value is lower than 0.25 (Figure 2): 2.48−3.42 Å for the $Li^{+1.0}Cl^{-1.0}$(aq) solution, 2.65−3.35 Å for the $Li^{+0.8}Cl^{-0.8}$(aq) solution, and 3.00−3.35 Å for NaCl(aq). These limits correspond roughly to the interchange regions discussed in section 3.3. (An example of a "discarded" configuration is seen in Figure 3, where molecule no. 4 leaves the first hydration shell at $t = 3.3$ ps.) Even if just one water molecule resides in this region, the configuration was given zero weight, while, for the complex to be classified as a 6-complex, for example, all six water molecules have to be present in the first hydration shell. Thus many more configurations are removed than what may be expected from the low $g(r)$ value in the intershell region. Altogether, some 12%, 24%, and 31% of the MD dumps were removed for the $Li^{+1.0}Cl^{+1.0}$, the $Li^{-0.8}Cl^{-0.8}$, and the NaCl solution, respectively.

For the remaining MD dumps, all water molecules were counted inside the limiting hydration sphere around the cation, i.e., 2.48 Å for $Li^{+1.0}$, 2.65 Å for $Li^{+0.8}$, and 3.00 Å for NaCl(aq). The resulting $P(n)$ histograms are shown in Figure 7. The most probable clean complex in the LiCl(aq) simulation is indeed the 6-coordinated one. There is also a tiny probability of finding a 5-coordinated complex. The most probable complex in the

TABLE 3: Volumes of Different Coordination Complexes for the 5-, 6-, and 7-Complexes for $Li^{+0.8}Cl^{-0.8}$(aq) and NaCl(aq)

	$\rho(r)$	Voronoi polyhedra	
complex type	vol. of complex (Å^3)	no. of complexes	vol. of complex (Å^3)
	$Li^{+0.8}Cl^{-0.8}$(aq)		
5	133.0	189	123.8
6	137.6	201	145.6
	NaCl(aq)		
6	171.9	201	162.0
7	181.8	202	183.6

NaCl(aq) solution is also the 6-coordinated one, followed by the 7-complexes, and by the 8-coordinated complexes. Since the 7-complex turns out to be more than half as common as the 6-complex, this makes it slightly disputable whether it is appropriate to call the 7-complex an "intermediate".

3.5. Activation Volumes. Activation volumes were determined for the 6-5-6 exchanges in our $Li^{+0.8}Cl^{-0.8}$(aq) solution and the 6-7-6 exchanges in the NaCl(aq) system. Two different methods were used. In the first method, we used cation−H $\rho(r)$ curves calculated separately for the 5- and 6-complexes [LiCl(aq)] or 6- and 7-complexes [NaCl(aq)]. In the other method, we calculated the volumes of the Voronoi polyhedra enclosing each molecule (see ref 29 and references therein).

Since the coordinating water molecules' hydrogen atoms are always directed outward, they were chosen to represent the outer boundary of the complexes. Our "$\rho(r)$ method" uses the cation-hydrogen local number density for water molecules in the first hydration shell. After removing the "nonpure" coordination complexes as described in section 3.4, each remaining cation−water complex was classified as an *n*-coordinated complex. It should be pointed out that since fewer exchanges occur for $Li^{+0.8}Cl^{-0.8}$(aq) than for NaCl(aq), the statistics for the 6-5-6 process are not as good, and the resulting $\Delta V^{\ddagger}$ value should therefore be interpreted with due caution. The average volumes of the 5-, 6-, and 7-complex types were calculated in several steps:

(i) Counting only the water molecules within the first hydration shell, the cation−hydrogen local number density, $\rho^{\text{first}}(r)$, was computed separately for the 5-, 6-, and 7-complex types, using the selected dumps, according to

$$\rho^{\text{first}}(r) = \frac{m^{\text{first}}(r)}{4\pi r^2 \Delta r}$$

Here, $m^{\text{first}}(r)$ is the number of first-shell hydrogens found in a spherical shell of radius r and thickness Δr centered on the cation. $\rho^{\text{first}}(r)$ thus goes to zero beyond the first shell of neighbors.

(ii) At regular distance intervals, the volume of a sphere with its radius set to the sum of the cation−hydrogen distance and the hydrogen covalent radius was constructed, $V(r + r_{\text{cov}})$.

(iii) The average volume was computed from the average volume of these spheres, weighted with $\rho^{\text{first}}(r)$:

$$\langle V \rangle = \frac{1}{N^{\text{first}}} \int_0^\infty V(r + r_{\text{cov}})\, \rho^{\text{first}}(r)\, 4\pi r^2\, dr$$

N^{first} is the total number of hydrogen atoms in the first hydration shell for each dump. The resulting volumes are given in the first column of Table 3. This whole procedure is exactly equivalent to computing the average volume of each complex type, in such a way that the volume of each individual complex is taken to be the average of the volumes of the $2 \cdot n$ spheres, arising from the n coordinating water molecules (Figure 8). This method works best the more symmetrical and "spherical" the complex is, like a regular octahedral complex. The method also would not work if the H atoms were almost homogeneously distributed in a spherical shell around the cation. In all four cases analyzed in Table 3, however, the H atoms are located in a rather thin shell around the cation (FWHH for the cation−H $g(r)$'s are equal to or less than 0.5 Å).

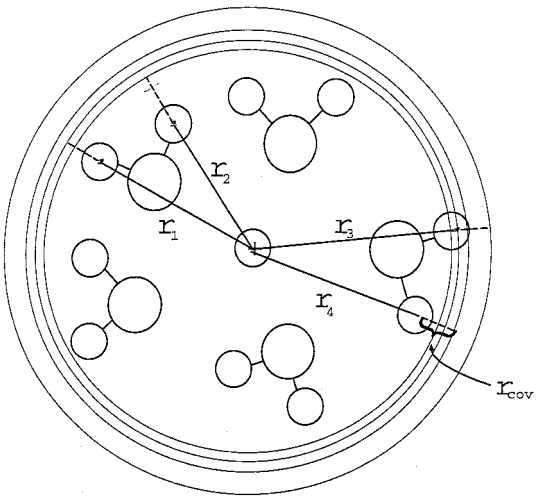

Figure 8. Illustration of how the average volume for the 5-complexes is calculated using the "$\rho(r)$ method". This picture shows one specific 5-complex. There are thus 10 cation−hydrogen distances involved (r_1, ..., r_{10}). Only four of these are marked in the picture. With each hydrogen we associate a sphere, with an outer limit equal to the cation−hydrogen distance plus the hydrogen covalent radius (r_{cov}). Ten spheres are thus constructed, with radii ($r_i + r_{\text{cov}}$), $i = 1, ..., 10$, respectively. Four of these are shown in the picture. The volume of the 5-complex in the picture is the average volume of the 10 constructed spheres: $V = (4\pi/3)\cdot[(r_1 + r_{\text{cov}})^3 + (r_2 + r_{\text{cov}})^3 + ... + (r_{10} + r_{\text{cov}})^3]/10$. The volume of the 5-complex type is the average of the volumes of many complexes such as this one. In practice, the calculation was done via the cation−hydrogen $\rho(r)$ functions, calculated separately for the 5-, 6-, and 7-complexes, as described in the text.

The method using Voronoi polyhedra is based on decomposing the volume of the MD box into a unique, space-filling set of polyhedra, which are centered on each molecule. The polyhedra are constructed so that their faces bisect the lines (vectors) connecting the given molecule with all its neighbors. The Voronoi polyhedron for the molecule is, then, the minimum-volume polyhedron so constructed. A two-dimensional example illustrating this scheme is shown in Figure 9. The volume of the complex is taken to be the sum of the component molecular/ionic polyhedra. The volume of a particular 7-complex, for example, is the sum of the volume of the cation polyhedron and the volumes of the seven water polyhedra belonging to the first-shell water molecules. The average volume for the 7-complex type is the average volume of all these 7-complexes found in our selected MD dumps.

Since the computation of Voronoi polyhedra is fairly time-consuming, only a rather small number of complexes were used for these calculations. The selected configurations were almost evenly spread out in time during the simulation. For the 5-, 6-, and 7-complexes, about 200 configurations were used, evenly spread out in time from the simulation dumps. The resulting volumes from the Voronoi polyhedra calculations are given in the last columns of Table 3.

The volume of a water molecule in the bulk was calculated from an MD simulation of pure TIP4P water at 300 K using

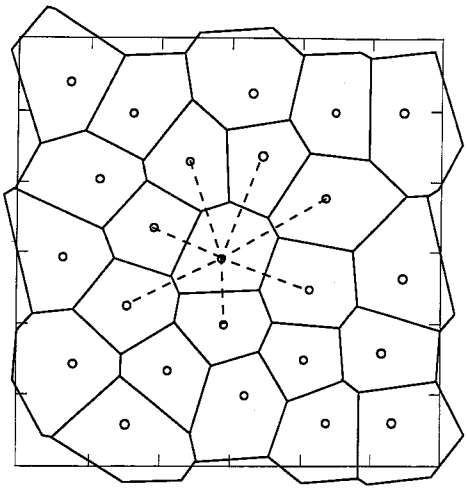

Figure 9. Two-dimensional construction of Voronoi polyhedra (polygons). Circles are molecular (or ionic) centers. The dashed lines connecting molecules are bisected by the faces (sides) of the polyhedra (polygons). See text.

the same number of water molecules as in the ionic solution simulations. The result was 29.9 Å^3/molecule. It is interesting to note that this pure water molecular volume is slightly larger than the average molecular Voronoi polyhedron volume calculated for the water molecules outside the second hydration shell in the ionic solutions, which come out to 29.0 Å^3 for NaCl(aq) and ∼29.3 Å^3 for $Li^{+0.8}Cl^{-0.8}$(aq). It is totally reasonable and not very surprising that electrosrestriction effects from the polarizing cations affect also the water molecules outside the second hydration shell.

The activation volumes for the exchange mechanisms can be calculated from the data in Table 3. With the Voronoi method we obtain the following results:

dissociative mechanism for $Li^{+0.8}Cl^{-0.8}$(aq):
volume of 6-complex: 145.6 Å^3
volume of 5-complex: 123.8 Å^3
volume of bulk water molecule: 29.9 Å^3
$\Delta V^{\ddagger} = (123.8 + 29.9) - 145.6 = 8.1$ Å^3/molecule $= 4.9$ cm^3/mol
associative mechanism for NaCl(aq):
volume of 6-complex: 162.0 Å^3
volume of 7-complex: 183.6 Å^3
volume of bulk water molecule: 29.9 Å^3
$\Delta V^{\ddagger} = 183.6 - (162.0 + 29.9) = -8.3$ Å^3/molecule $=$ -5.0 cm^3/mol

Activation volumes were calculated in the same way for the "$\rho(r)$ method" with the results 15.2 cm^3/mol for the dissociative mechanism for $Li^{+0.8}Cl^{-0.8}$(aq) and -12.0 cm^3/mol for the associative mechanism for NaCl(aq). As stated in the Introduction, a negative sign for $\Delta V^{\ddagger}_{expt}$ is commonly interpreted as evidence for an associative mechanism, and a positive sign as evidence of a dissociative mechanism. Our calculations show that this molecular-level interpretation of the sign of the activation volume is reasonable. The two different methods both indicate that in a 6-7-6 process the average volume of the intermediate complex is *smaller* than the sum of the volumes of a 6-complex and a bulk water molecule. Similarly the simulations show that in a 6-5-6 process the sum of the average volumes of the intermediate complex and a bulk water molecule is *larger* than the volume of the 6-complex. These results represent knowledge that is difficult to obtain by other methods.

In summary, the mechanistic picture of the exchange process in our two alkali chloride solutions is the following. For NaCl(aq) the exchange process is predominantly of an associative character with a $\Delta V^{\ddagger}$ value somewhere between -5 and -12 cm^3/mol. For both our LiCl(aq) solutions the exchange process is predominantly of a dissociative character, with a $\Delta V^{\ddagger}$ value for $Li^{+0.8}Cl^{-0.8}$(aq) somewhere between $+5$ and $+15$ cm^3/mol. Although no experimental activation volumes have been reported in the literature for water exchange around Li^+ or Na^+, we can compare with the reported activation volumes for the transition metal ions, which are -4.1 for V^{2+}, -5.4 for Mn^{2+}, $+3.8$ for Fe^{2+}, $+6.1$ for Co^{2+}, and $+7.2$ cm^3/mol for Ni^{2+}.[17] The magnitudes of all these activation volumes are of the same order as our resulting volumes for the alkali ions.

Summary

Most of the exchange processes can be classified in terms of D, I_D, I, I_A, and A. Several exceptions are found in the NaCl(aq) solution, however.

The water exchanges occur considerably more frequently around the sodium ion than around the lithium ion. This is consistent with the fact that the softer and larger sodium ion does not bind the water molecules as strongly as the harder and smaller lithium ion.

The exchange mechanisms are different for the two ions. There are predominantly associative exchanges (A) around the sodium ion and dissociative ones (D and I_D) around the lithium ion.

The average lifetimes of the predominant intermediate complexes, $[Na(H_2O)_7]^+$ and $[Li(H_2O)_5]^{+0.8}$, are about equally long, 0.6−0.7 ps. The spread in lifetimes for the intermediate complexes is large in all three solutions, typically in the range from 0 to 2 ps and occasional lifetimes as long as 5 ps.

The activation volume for the 6-7-6 exchange process in NaCl(aq) was calculated as the volume difference between the volume of the 7-complex and the sum of the volumes of the 6-complex and a bulk water molecule. Two different methods were used. One method was based on cation−H $\rho(r)$ curves calculated separately for 6- and 7-complexes; the other computes Voronoi polyhedra around all particles. Both methods gave a negative sign for$\Delta V^{\ddagger}$. Corresponding calculations for the 6-5-6 exchanges in $Li^{+0.8}Cl^{-0.8}$(aq) gave a positive sign with both methods. This supports a molecular-level interpretation of $-RT\cdot(\partial \ln k)/\partial P$ as reflecting the difference in volumes between the transition state and the initial complex and supports the connection between a negative $\Delta V^{\ddagger}$ and an associative process, and also between a positive $\Delta V^{\ddagger}$ and a dissociative process. The two methods gave a large spread in values, however, but all lie in the range that has been observed experimentally for other metal cations.

Acknowledgment. This work has been supported by the Swedish Natural Science Research Council (NFR), which is gratefully acknowledged. Many of the calculations underlying this work were performed by Messieurs Daniel Spångberg and Harald Tepper; their help is much appreciated.

References and Notes

(1) Ohtaki, H.; Radnai, T. Structure and Dynamics of Hydrated Ions. *Chem. Rev.* **1993**, *93*, 1157.
(2) Cotton, F. A.; Wilkinson, G. *Advanced Inorganic Chemistry*; 4th ed.; John Wiley & Sons: New York, 1980; pp 1188−1189.
(3) Friedman, H. L. *Chem. Scr.* **1985**, *25*, 42.
(4) Veillard, H. *J. Am. Chem. Soc.* **1977**, *99*, 7194.
(5) Probst, M. M.; Hermansson, K. *J. Chem. Phys.* **1992**, *96*, 8995.
(6) Åkesson, R.; Pettersson, L. G. M.; Sandström, M. Siegbahn, P. E. M.; Wahlgren, U. *J. Phys. Chem.* **1993**, *97*, 3765.
(7) Åkesson, R.; Pettersson, L. G. M.; Sandström, M.; Wahlgren, U. *J. Am. Chem. Soc.* **1994**, *116*, 8705.
(8) Rotzinger, F. P. *J. Am. Chem. Soc.* **1996**, *118*, 6760.
(9) Impey, R. W.; Madden, P. A.; McDonald, I. R. *J. Phys. Chem.* **1983**, *87*, 5071.

(10) Guàrdia, E.; Padro, J. A. *J. Phys. Chem.* **1990**, *94*, 6049.
(11) Lee, S. H.; Rasaiah, J. C. *J. Chem. Phys.* **1994**, *101*, 6964.
(12) Lee, S. H.; Rasaiah, J. C. *J. Phys. Chem.* **1996**, *100*, 1420.
(13) Obst, S.; Bradaczek, H. *J. Phys. Chem.* **1996**, *100*, 15677.
(14) Kowall, Th.; Foglia, F.; Helm, L.; Merbach, A. E. *J. Am Chem. Soc.* **1995**, *117*, 3790.
(15) Kowall, Th.; Foglia, F.; Helm, L.; Merbach, A. E. *Chem. Eur. J.* **1996**, *2*, 235.
(16) Rey, R.; Hynes, J. T. *J. Phys. Chem.* **1996**, *100*, 5611.
(17) Rey, R.; Hynes, J. T. *J. Phys.: Condens. Matter* **1996**, *8*, 9411.
(18) Spångberg, D.; Wojcik, M.; Hermansson, K. *Chem. Phys. Lett.* **1997**, *276*, 114.
(19) Burgess, J. *Ions in solution, basic principles of chemical interactions*; Ellis Horwood Ltd.: New York, 1988.
(20) *Studies in Inorganic Chemistry 7: Inorganic High Pressure Chemistry, Kinetics and Mesurements*; van Eldik, R., Ed.; Elsevier: Amsterdam, 1986.
(21) Morita, T.; Ladanyi, B. M.; Hynes, J. T. *J. Phys. Chem.* **1989**, *93*, 1386.
(22) Anderson, H. C. *J. Chem. Phys.* **1980**, *72*, 2384.
(23) Nosé, S. *J. Chem. Phys.* **1984**, *81*, 511. Hoover, W. G. *Phys. Rev. A* **1985**, *31*, 1695.
(24) Nosé, S.; Klein, M. L. *Mol. Phys.* **1983**, *50*, 1055.
(25) Jorgensen, W. L.; Chandrasekhar, J.; Madura, J. D.; Impey, R. W.; Klein, M. L. *J.Chem. Phys.* **1983**, *79*, 926.
(26) Bounds, D. G. *Mol. Phys.* **1985**, *54*, 1335.
(27) Sangster, M. J. L.; Atwood, R. M. *J. Phys. C: Solid State Phys.* **1978**, *11*, 1541.
(28) Hermansson, K.; Tepper, H. L. Unpublished results, 1995.
(29) Finney, J. L. *Proc. R. Soc. London A* **1970**, *319*, 479−495.
(30) Aylward, G.; Findlay, T. *SI Chemical Data*, 3rd ed.; John Wiley & Sons: New York, 1994.